Reaction mechanism and thermoelectric properties of In0:22Co4Sb12 prepared by magnesiothermy

Sylvain Le Tonquesse, Eric Alleno, Valérie Demange, Carmelo Prestipino, Olivier Rouleau, Mathieu Pasturel

Reaction mechanism and thermoelectric properties of $In_{0.22}Co_4Sb_{12}$ prepared by magnesiothermy

Sylvain Le Tonquesse[a], Éric Alleno[b], Valérie Demange[a], Carmelo Prestipino[a], Olivier Rouleau[b], Mathieu Pasturel[a,]

[a]*Univ Rennes, CNRS, Institut des Sciences Chimiques de Rennes - UMR6226, F-35000, Rennes, France*
[b]*Université Paris-Est, Institut de Chimie et des Matériaux Paris-Est, UMR 7182 CNRS - UPEC, 2 rue H. Dunant, 94320 THIAIS, France*

Abstract

The magnesioreduction synthesis of $In_{0.22}Co_4Sb_{12}$ with high In-rattler concentration from Sb_2O_4 and In-doped Co_3O_4 precursors is reported. This process directly yields a submicronic powder in a single step of 96 h at 810 K. The reaction mechanism has been investigated by stopping the reaction every 12 h and quantifying the existing phases by X-ray diffraction and Rietveld refinements. The precursors are first reduced in CoO and Sb_2O_3 lower oxides, then form $CoSb_2O_6$ and $CoSb_2O_4$ intermediates which are finally reduced in $In_xCo_4Sb_{12}$. A powder with 350 nm average size and mostly composed of In-filled skutterudite phase with composition close to $In_{0.17}Co_4Sb_{12}$ is obtained. Upon spark plasma sintering, small residual amount of InSb reacts with the skutterudite matrix to form a single-phase densified pellet with composition close to $In_{0.22}Co_4Sb_{12}$. The resulting densified material with 1.8 μm average grain size shows a figure-of-merit ZT_{max} of 0.95 at 750 K.

Keywords: Skutterudites; Magnesioreduction synthesis; Reaction mechanism; Thermoelectric properties.

*mathieu.pasturel@univ-rennes1.fr; Institut des Sciences Chimiques de Rennes, Campus de Beaulieu, bat. 10A, 263 avenue Général Leclerc, 35042 Rennes Cedex, France

1. Introduction

Thermoelectric (TE) materials enable the direct conversion of heat into electricity through the Seebeck effect. The conversion efficiency is directly related to the figure-of-merit ZT defined as:

$$ZT = \frac{\alpha^2}{\rho\,(\kappa_L + \kappa_e)}\,T \tag{1}$$

with α the Seebeck coefficient, ρ the electrical resistivity, κ_L and κ_e the lattice and electronic contributions to the total thermal conductivity κ and T the temperature. $CoSb_3$-based skutterudites are well-known TE materials with a band gap of about 0.2 eV [1]. They are considered as promising candidates for mid-temperature (600 - 800 K) TE applications because of their excellent electronic properties, good mechanical properties and relatively abundant constituting elements. Large power factors, $PF = \alpha^2/\rho$, reaching 4 - 5 mW m^{-1} K^{-2} can be obtained for compositions with optimized charge carrier concentration. In order to achieve high ZT, the intrinsic high thermal conductivity ($\approx$ 9 W m^{-1} K^{-1} at 298 K for $CoSb_3$ [2]) must be reduced as much as possible without simultaneously degrading the electronic properties. This can be effectively done by partially filling the empty isocahedral voids of the structure with rare-earth, alkaline metal or III - IV group elements [1]. The additional mass contrast induced by the partial occupancy as well as the 'rattling' behavior of the filling atoms in the oversized voids effectively scatter acoustic heat-carrying phonons. For example, lattice thermal conductivities as low as 1 - 2 and $\approx$ 0.5 W m^{-1} K^{-1} were reported for single Ba-, Ca- and Yb-filled [3, 4, 5] and nanostructured multi-filled skutterudites [6], respectively.

Indium is among the most studied filler atom for *n*-type skutterudites because (i) it acts as an electron donor enabling large increase of PF and (ii) it

efficiently reduces κ_L due to its heavy atomic mass. While some controversy exists about its true solubility limit ($0.16 < x < 0.27$) [7, 8, 9], all authors agree that the best performances are obtained by maximizing the In concentration [2, 10]. ZT_{max} of about 1.1 are usually reported for materials with composition close to $In_{0.25}Co_4Sb_{12}$ and synthesized by conventional fusion/solidification processes [11, 2]. However, due to the peritectic formation of $CoSb_3$, long annealing (> 100 h) at high temperature (1100 K) are required to form a single phase product. In addition, the ingots are composed of microns sized grains which need to be reduced by milling in order to reduce κ_L. κ reduction were attempted using such conventional approach by *in situ* formation of InSb nanoprecipitates [12, 13, 14] or by designing mesostructured materials with oxide nanoinclusions [11, 15]. These additional annealing and milling steps, to be performed under unreactive atmosphere, cost time and energy cost and could become an obstacle to the large scale production of this material.

Alternative processes have been developed to overcome the problematic synthesis of this material. For example, hydrothermal [16, 17] or melt-spinning/reactive spark plasma sintering approaches [18] have been adapted to the synthesis of nanostructured $In_xCo_4Sb_{12}$ with high concentration of interfaces between the grains and lattice thermal conductivity as low as 1.5 W m^{-1} K^{-1}. Most importantly, these alternative routes do not require any post-reaction annealing which considerably speed up the synthesis. However, nanostructured materials often suffer from largely higher electrical resistivity usually attributed to the lower density of the sintered materials [19, 16] or to the enhanced charge carriers scattering at the numerous interfaces/defects, considerably reducing the beneficial effect of the microstructure on *ZT*.

In a previous article [20], we reported a new magnesioreduction synthesis

for $In_xCo_4Sb_{12}$ with x = 0.13 according to the reaction:

$$2\,(\mathrm{In})Co_3O_4 + 9Sb_2O_4 + 44Mg \xrightarrow[96h]{810K} 6(\mathrm{In})CoSb_3 + 44MgO \qquad (2)$$

This process, also applied to the production of TE-silicides [21], possesses many advantages such as the direct synthesis of high purity skutterudite powders with submicronic average grain sizes without additional long annealing or milling step, high yield, relatively low reaction temperature and the use of cheap and air-stable oxide precursors. Moreover, magnesiothermy is already used to industrially produce metals via the Kroll [22] or Ames [23] processes and offer thus interesting scalability perspectives. In the present article, this magnesioreduction process is adapted to the synthesis of saturated $In_{0.22}Co_4Sb_{12}$. The discussion will mainly focus on the comprehension of the reaction mechanism which was investigated by X-ray diffraction (XRD). Finally, the thermoelectric properties were measured and compared to those of reference samples from the literature.

2. Experimental procedures

The detailed procedure for the magnesioreduction synthesis of In-filled skutterudites according to reaction (2) is described in a previous work [20]. For preparation of the '$In_{0.18}Co_{2.81}O_4$' precursor, stoichiometric amounts of $CoCl_2{\cdot}6H_2O$ (Prolabo, 99.9 %) and $In(NO_3)_3{\cdot}xH_2O$ (home-made by dissolving In in concentrated HNO_3) are dissolved in distilled water and then precipitated using NaOH. The precipitate is washed with water and ethanol several times, dried at 363 K and calcined at 723 K for 4 h in air. XRD pattern (fig. SI 1) shows broad diffraction peaks corresponding to Co_3O_4 and In_2O_3. Rietveld refinement converges to a lattice parameter a = 8.137(9) Å significantly larger than for pristine Co_3O_4 (a = 8.076 Å [24]) suggesting the insertion of In in the structure [25]. The pres-

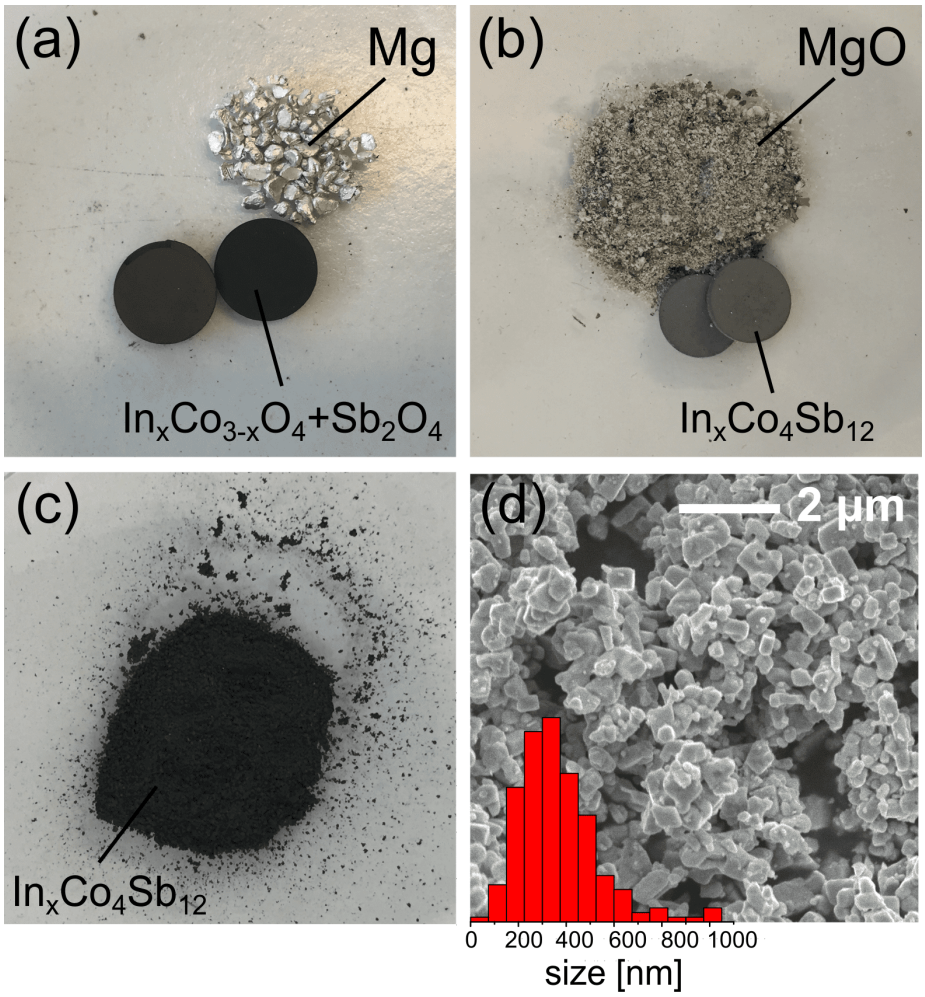

Figure 1: Pictures of (a) the reaction precursors, (b) reaction products after 96 h at 810 K and (c) crushed as-synthesized $In_xCo_4Sb_{12}$ pellets. (d) Secondary electron SEM image of the as-synthesized powder with histogram showing the grain size distribution.

ence of remaining In_2O_3 indicates that the solubility limit has been reached. A mixture of this precursor and Sb_2O_4 (Sigma-Aldrich, 99.995 %) with 1:5.4 molar composition, required to counterbalance the loss of antimony by evaporation during the MR process and obtain phase pure samples [20], is thoroughly milled in an agate mortar. The oxide mixture is cold-pressed at 250 MPa into Ø 10 mm pellets with about 2 mm height (fig. 1a). The pellets (usually 2 stacked on top

of each other) are placed with Mg chunks (2 - 3 % excess) in a clamped Mo crucible. The crucible is heated to 810 K for 96 h under protective Ar atmosphere before being cooled down to room temperature. After the reaction, the skutterudite remains in the shape of compact pellets and can easily be separated from the loose MgO (fig. 1b). The powder (fig. 1c,d) is then spark plasma sintered (FCT HP-D-10 system) in Ø 10 mm graphite dies at 1000 K and 66 MPa for 10 min.

Powder X-ray diffraction was performed on a Bruker D8 Advance diffractometer in the θ-2θ Bragg-Brentano geometry working with a monochromatized Cu Kα_1 radiation (λ = 1.5406 Å), equipped with a LynxEye detector which enables photon energy discrimination around 20 %, thus reducing the cobalt fluorescence signal. Lattice parameters and phase fractions were determined by the Rietveld method using the FullProf software [26]. Scanning electron microscopy (SEM) images and energy dispersive spectroscopy (EDS) were performed on a JEOL JSM 7100 F microscope equipped with an Oxford EDS SDD X-Max spectrometer. Transport properties measurements were carried out using a home-made apparatus described elsewhere [27]. Thermal diffusivity measurements were performed using a Netzsch LFA 457 equipment under Ar atmosphere. The thermal conductivity was determined from $\kappa = D\ C_p\ d$ with D the thermal diffusivity, C_p the specific heat of the sample calculated using the Dulong-Petit law and d the sample density determined by the Archimede method in absolute ethanol.

3. Results and discussion

3.1. Reaction mechanism and skutterudite characterizations

$In_xCo_4Sb_{12}$ (targeted x = 0.25) has been synthesized, along with some InSb and Sb impurities, from Sb_2O_4 and In-doped Co_3O_4 after 96 h heat treatment

at 810 K in presence of Mg. To elucidate the reaction mechanism, the synthesis was repeated several times and stopped every twelve hours. Each time, the phases in the samples were quantified by the Rietveld method and their relative concentrations are represented in fig. 2. Figure 3 shows some selected XRD patterns while all refined patterns and parameters can be found in supplementary information (fig. SI 2, tables SI. 1 - 9). Up to 6 different phases have been identified in some patterns indicating a complex reaction mechanism. The full reduction of the precursors is realized in three steps: (i) the partial reduction of the precursors in lower oxides (0 h - 24 h), (ii) the formation of $CoSb_2O_6$ and $CoSb_2O_4$ intermediates (0 h - 48 h) and (iii) the complete reduction of the intermediates and the formation of $In_xCo_4Sb_{12}$ (38 h - 96 h).

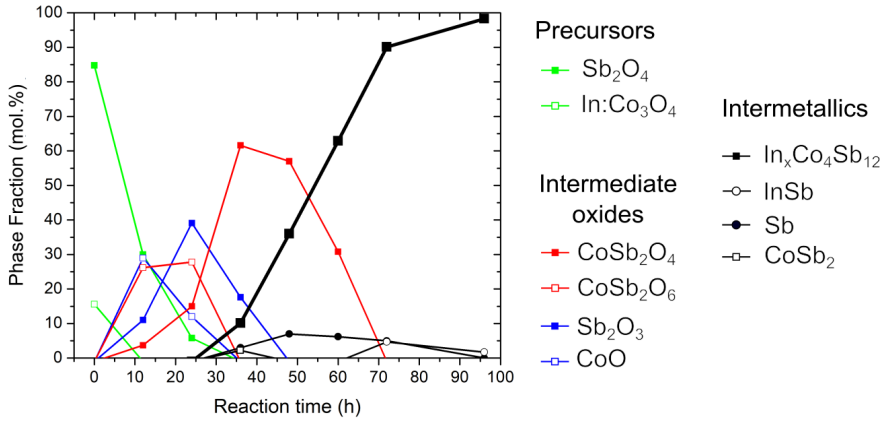

Figure 2: Evolution of the sample composition during the magnesioreduction synthesis of $In_xCo_4Sb_{12}$, determined by the Rietveld method, as a function of the reaction time. In the present case and according to [28], the relative standard deviation on the concentrations are considered to be well below 5 %.

The precursors mixture is initially composed of Sb_2O_4 [Sb^{3+}, Sb^{5+}] and $In:Co_3O_4$ [Co^{2+}, Co^{3+}]. After 24 h at 813 K, $In:Co_3O_4$ and Sb_2O_4 almost completely disappeared. Instead, freshly formed CoO [Co^{2+}] and Sb_2O_3 [Sb^{3+}] represent almost 50 % of the reaction media. This suggests the partial reduction of

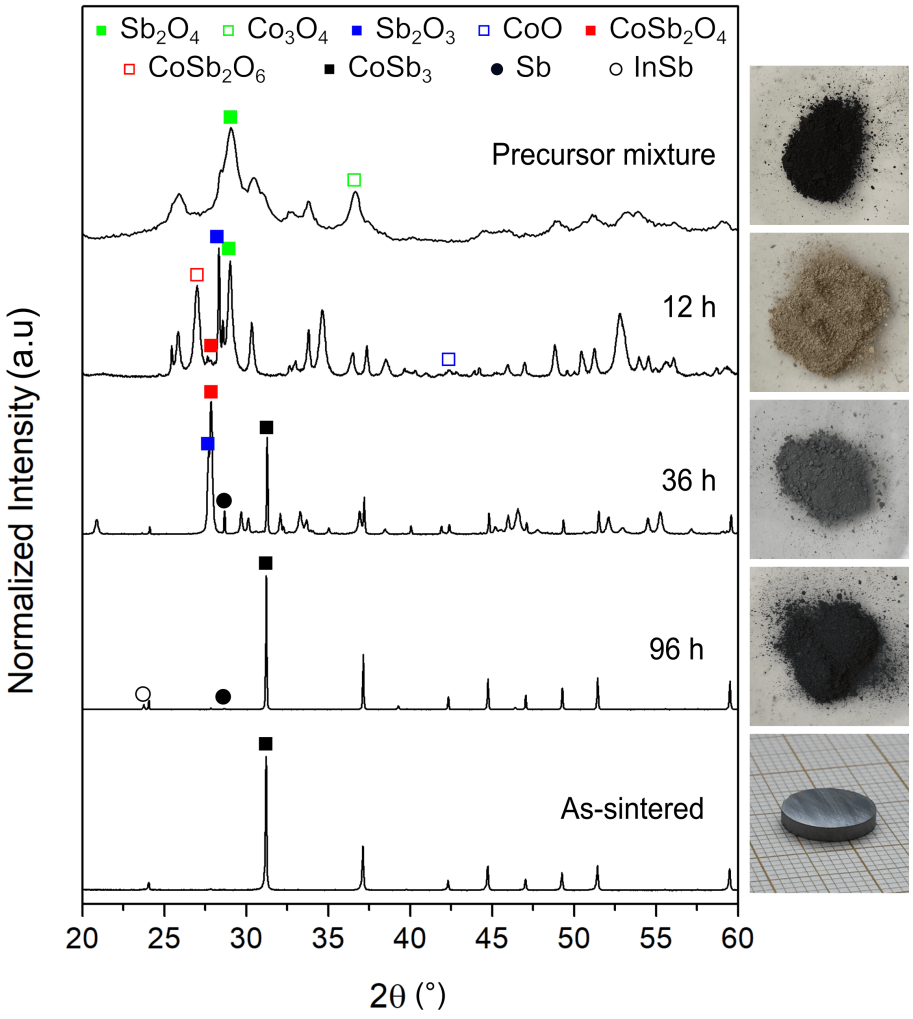

Figure 3: XRD patterns of the $In_xCo_4Sb_{12}$ magnesioreduction synthesis after 0 h, 12 h, 36 h, 96 h reaction time and after spark plasma sintering. The symbols indicate the most intense reflections of each constituting phases. The images shows the evolution of the product color with the reaction time.

the precursors in lower oxides by Mg according to the reactions:

$$Co_3O_4 + Mg \xrightarrow[12h]{810K} 3\,CoO + MgO \qquad \Delta G_r(810\ \mathrm{K}) = \text{-}512.3\ \mathrm{kJ\ mol^{-1}}[29] \quad (3)$$

$$Sb_2O_4 + Mg \xrightarrow[12h]{810K} Sb_2O_3 + MgO \qquad \Delta G_r(810\ K) = \text{-}396.4\ kJ\ mol^{-1}\ [29] \quad (4)$$

These reductions are thermodynamically possible at 810 K as indicated by the large negative Gibbs free energy of reaction. In addition, $CoSb_2O_6$ [Co^{2+}, Sb^{5+}] ($P4_2/mnm$) and $CoSb_2O_4$ [Co^{2+}, Sb^{3+}] ($P4_2/mbc$) ternary intermediates are formed most likely by solid state reactions between the various binary oxides in presence. This is supported by several works reporting the synthesis of these mixed oxides by conventional solid-state reaction starting from CoO and Sb_2O_3/Sb_2O_5 powders between 973 and 1073 K [30, 31, 32].

After 36 h, no trace of $CoSb_2O_6$ remains in the XRD pattern (fig. 3) and $CoSb_2O_4$ is the major phase representing 60 mol.% of the sample. According to the simultaneous decrease of $CoSb_2O_6$ and increase of $CoSb_2O_4$ contents, one might expect $CoSb_2O_4$ to be formed from the reduction of $CoSb_2O_6$ according to:

$$CoSb_2O_6 + 2\,Mg \longrightarrow CoSb_2O_4 + 2\,MgO \quad (5)$$

More interestingly, skutterudite starts forming ($\approx$ 10 %) and the lattice parameter a = 9.0384(8) Å corresponds well to $In_xCo_4Sb_{12}$ with low In-content (x $<$ 0.05) [7, 8]. At this point of the reaction, Sb^{5+} and Co^{3+} are no more present in the reaction media and Sb^{3+} and Co^{2+} are consecutively reduced in metallic Co and Sb.

The complete reduction of $CoSb_2O_4$ and Sb_2O_3 into $CoSb_3$ takes another 36 hours according to:

$$2\,CoSb_2O_4 + Sb_2O_3 + 11Mg \longrightarrow 2\,CoSb_3 + 11MgO \quad (6)$$

Traces of InSb appear on the diffraction patterns after 72 h. We hypothesize that In was solubilized in $CoSb_2O_4$ because (i) the formation of InSb corresponds to the total reduction of $CoSb_2O_4$, (ii) the refined lattice parameters of the latter, a = 8.5078(5) Å and c = 5.9316(5) Å, are significantly larger than literature data, a = 8.49285(7) Å and c = 5.92449(5) Å [30] and (iii) other elements such as Pb^{2+} can substitute Sb to a great extent in $CoSb_2O_4$ [30]. In presence of InSb, the lattice parameter of In_xCoSb_3 increases from 9.0384(2) Å after 48 h to 9.04872(4) Å after 96 h. This can be explained by the insertion of In in the $CoSb_3$ structure according to:

$$Co_4Sb_{12} + xInSb \longrightarrow In_xCo_4Sb_{12} + xSb \tag{7}$$

The slow diffusion of In in $CoSb_3$ was already stressed out by Grytsiv *et al.* [8]. After 96 h, the reaction media is mostly composed of $In_xCo_4Sb_{12}$ with a = 9.04872(4) Å which corresponds to x = 0.17 - 0.18 [7, 8] and of a small amount of InSb ($\approx$ 4 mol.%) and Sb ($\approx$ 2 mol.%). No traces of MgO or Mg containing compound are visible at any time on the diffraction patterns. For this reason, we hypothesize that the reduction reactions occur *via* the slow oxidation of the Mg chunks by the equilibrium O_2 vapor pressure of the oxides. This is consistent with the general aspect of the Mg chunks between 24 h to 48 h which are clearly oxidized at the surface (powdery and white) but remain metallic and relatively shinny in the core.

The as-synthesized powder was spark plasma sintered to obtain pellets with 97 % relative density. The XRD pattern of the as-sintered pellet (fig. 3) is fully indexed with the skutterudite structure type. Rietveld refinement results in a lattice parameter a = 9.0527(2) Å which is significantly larger than that of the as-synthesized powder. Along with the disappearance of the InSb secondary phase, whose melting point (789 K) is lower than the sintering temperature, this

suggests that InSb reacts with the skutterudite matrix during the sintering step thus increasing the inserted In content. According to literature data, this lattice parameter corresponds to a true $In_xCo_4Sb_{12}$ composition close to x = 0.20 - 0.22 [7, 8]. The scenario is very similar to the synthesis of $In_{0.13}Co_4Sb_{12}$ where about 20 % of In was inserted in the structure during the sintering step [20].

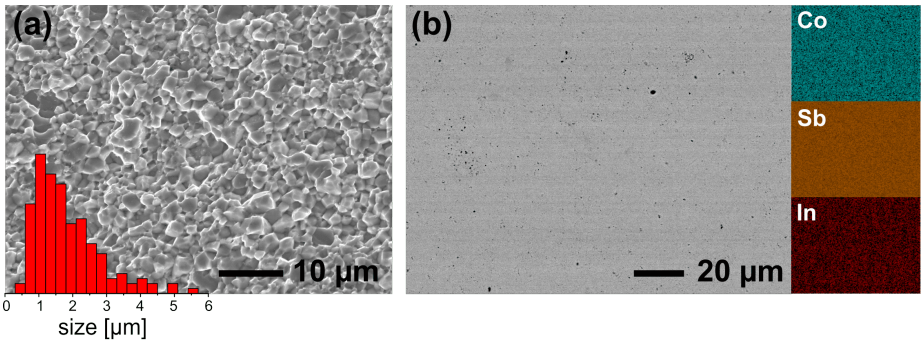

Figure 4: (a) Secondary electron SEM image of a broken cross-section of a densified $In_{0.22}Co_4Sb_{12}$ pellet and histogram showing the distribution of the apparent grain size. (b) Backscattered electron SEM image and corresponding EDS elementary mappings of the pellet polished surface.

Backscattered electron image and EDS mapping of the pellet (fig. 4b) reveal homogeneous chemical composition. Indium filling fraction could however not be accurately quantified by EDS because of its low concentration and the partial overlapping of the In L_α and the intense Sb L_α peaks. The magnesioreduction synthesis of $In_{0.30}Co_4Sb_{12}$ was also attempted but InSb in excess leaked out of the die during sintering and the resulting skutterudite lattice parameter remained close to a = 9.053 Å. As a result, $In_{0.22}Co_4Sb_{12}$ would be the In-richest composition accessible by magnesioreduction synthesis in these reaction conditions. It is in agreement with the solubility limit usually reported for In-filled $CoSb_3$ prepared by conventional melting/annealing [8] or solid state diffusion [33] syntheses. The SEM secondary electron image of the broken cross-section of a pellet is shown in fig. 4a. The microstructure is typical for magnesioreduced skutterudite with well-faceted grains and size distribution characterized

by an average value of 1.8 μm. The present grain size is significantly larger than our previous work [20]. This is mostly attributed to the 90 K higher sintering temperature found necessary to complete the reaction. Also the higher content of liquid InSb might have favored grain growth by accelerating matter transport during the sintering [34].

3.2. Thermoelectric properties

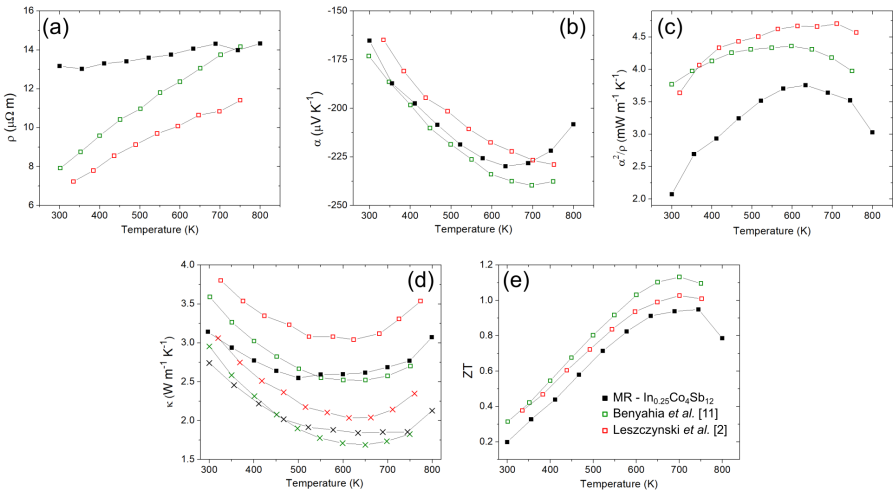

Figure 5: High-temperature dependence of (a) the electrical resistivity, (b) Seebeck coefficient, (c) power factor, (d) total (squares) and lattice (crosses) thermal conductivities and (e) figure-of-merit of $In_{0.22}Co_4Sb_{12}$ synthesized by magnesioreduction (filled black squares) along with literature data for $In_{0.25}Co_4Sb_{12}$ taken from [11] (green empty squares) and $In_{0.28}Co_4Sb_{12}$ taken from [2] (red empty squares).

The thermoelectric properties of $In_{0.22}Co_4Sb_{12}$ are shown in fig. 5 and compared to data from the literature on compounds with similar compositions. Data reported by Benyahia *et al.* [11] and Leszczynski *et al.* [2] were obtained for materials synthesized by melting/annealing/sintering method. Although the Seebeck coefficient of our sample compares well to literature data, the resistivity is more elevated, especially near room temperature. As a direct consequence, the PF_{max} is 7 to 20 % lower at 750 K. Despite its apparent purity and density, small cracks appeared on our sample upon thermal cycles that could explain

the higher measured resistivity. Such deterioration is attributed to the melting around 800 K [8] during the measurement cycle of small residual amount of InSb usually observed at the grain boundaries of saturated In-filled skutterudite [12, 35]. However, the In content in the structure remains constant as indicated by the similar lattice parameter, a = 9.0520(3) Å, determined after the thermoelectric characterization.

The room temperature thermal conductivity of MR sample is about 3.2 W m^{-1} K^{-1} and reaches its minimum value of 2.6 W m^{-1} K^{-1} in the 450 - 650 K range. The simultaneous decrease of α and upturn of κ at about 650 K is attributed to the bipolar effect *i.e.* to the contribution of two types of charge carriers to the material transport properties. The lattice thermal conductivity was determined by subtracting κ_e to κ and κ_e was calculated using the the Wiedemann-Franz law κ_e = L T/ρ with L taken from [2] as 1.7 10^{-8} W Ω K^{-2}. The κ_L of the magnesiosynthesized sample agrees with the lower κ_L values of the literature over the entire temperature range. No significant decrease of κ_L is measured at room temperature contrary to our previous work on $In_{0.13}Co_4Sb_{12}$ certainly because of the larger average grain size, 1.8 μm vs. 600 nm, respectively, and the stronger influence of the rattlers over the mesostructure at such elevated concentration. As a consequence of the lower *PF*, a ZT_{max} of 0.95 at 750 K is obtained which remains 5 and 15 % lower than the reference samples made by conventional melting/annealing process.

Further comparison of the MR-materials performance with literature data is not a straightforward task as long as the TE properties of In-filled skutterudites strongly depends on the precise In-content inserted in the cages up to its solubility limit [9, 33, 13, 36]. In the present case, we confirm that increasing the In-content from 0.13 [20] to 0.22 in the MR-samples decreases the thermal conductivity and increases the ZT_{max} from 0.75 to 0.95. Oversaturating In in

$CoSb_3$ induces the formation of InSb and/or $CoSb_2$ (nano)precipitates that are playing a significant role in decreasing the thermal conductivity and improving the ZT_{max} of these composite materials [37, 38, 39, 40]. MR-$In_{0.22}Co_4Sb_{12}$ do not show the presence of such precipitates after spark plasma sintering. The measured TE properties can thus be considered as intrinsic to the material and slightly deteriorated by the microcracks appearing in the pellets during physical properties measurements. The submicron particle size distribution obtained after magnesioreduction corresponds well to that reported by Benyahia *et al.* on mesostructured $ZT = 1.4$ $In_{0.25}Co_4Sb_{12}$. Unfortunately, the grain growth induced during sintering cancels this microstructural feature and both thermal conductivity and figure-of-merit are much closer from those obtained by fusion-solidification-long term annealing [2, 18] or most recently by scanning laser melting for higher In-content [41]. Nevertheless, our ZT value is most of the time higher than those reported after solid state diffusion [39, 42, 43] or HPHT technique [44]. Improving the SPS step to limit the grain growth, stabilizing $In_{0.22}Co_4Sb_{12}$/InSb nanocomposites or trying to form multifilled skutterudites by magnesiothermy are the perspectives of this work.

4. Conclusions

The investigation of the reaction mechanism for the magnesioreduction synthesis of In-filled skutterudite from Sb_2O_4 and In-doped Co_3O_4 evidenced a complex scenario involving intermediate species: CoO, Sb_2O_3, $CoSb_2O_6$ and $CoSb_2O_4$. The formation of $CoSb_3$ precedes the insertion of In-rattler in the cage. After spark plasma sintering, the resulting material is single phase skutterudite with composition close to $In_{0.22}Co_4Sb_{12}$ which corresponds to the In-richest composition which could be synthesized by this technique in these conditions. A ZT_{max} of 0.95 is measured at 750 K due to limited *PF* resulting from elevated ρ caused by microcracks appearing in the pellets. In addition to im-

portant energy and time saving, the relatively mild reaction conditions used in this process prevent high Mg vapors pressure inside the reactor thus avoiding the formation of deleterious Mg-containing side-products which often limits the up-scaling perspectives of magnesioreduction processes. Finally, the knowledge gained on the reaction mechanism will be a precious help for the development of optimized reaction conditions (multi-step heat treatment, mixed oxide precursors) enabling the insertion of other filler atoms (*e.g.* Ba, rare earths elements) whose respective oxides are often too stable to be reduced by Mg in the present reaction conditions.

Acknowledgements

Loic Joanny and Francis Gouttefangeas are acknowledged for SEM images and EDS analyses performed on the CMEBA platform belonging to the ScanMAT unit (UMS 2001, University of Rennes 1) which received a financial support from the European Union (CPER-FEDER 2007-2014).

Declaration of interest

The authors declare no conflict of interest.

References

[1] G. Rogl, P. Rogl, Skutterudites, a most promising group of thermoelectric materials, Curr. Opin. Green Sustainable Chem. 4 (2017) 50–57.

[2] J. Leszczynski, V. D. Ros, B. Lenoir, A. Dauscher, C. Candolfi, P. Masschelein, J. Hejtmanek, K. Kutorasinski, J. Tobola, R. I. Smith, C. Stiewe, E. M*ü*ller, Electronic band structure, magnetic, transport and thermodynamic properties of In-filled skutterudites $In_xCo_4Sb_{12}$, J. Phys. D: Appl. Phys. 46 (2013) 495106.

[3] X. Li, Q. Zhang, Y. Kang, C. Chen, L. Zhang, D. Yu, Y. Tian, B. Xu, High pressure synthesized Ca-filled $CoSb_3$ skutterudites with enhanced thermoelectric properties, J. Alloys Compd. 677 (2016) 61–65.

[4] Y. Kang, F. Yu, C. Chen, Q. Zhang, H. Sun, L. Zhang, D. Yu, Y. Tian, B. Xu, High pressure synthesis and thermoelectric properties of Ba-filled $CoSb_3$ skutterudites, J. Mater. Sci.: Mater. Electron. 28 (2017) 8771–8776.

[5] G. S. Nolas, M. Kaeser, R. T. Littleton, T. M. Tritt, High figure of merit in partially filled ytterbium skutterudite materials, Appl. Phys. Lett. 77 (2000) 1855.

[6] G. Rogl, A. Grytsiv, K. Yubuta, S. Puchegger, E. Bauer, C. Raju, R. Mallik, P. Rogl, In-doped multifilled n-type skutterudites with ZT = 1.8, Acta Mater. 95 (2015) 201–211.

[7] Y. Tang, Y. Qiu, L. Xi, X. Shi, W. Zhang, L. Chen, S.-M. Tseng, S. wen Chend, G. J. Snyder, Phase diagram of In-Co-Sb system and thermoelectric properties of In-containing skutterudites, Energy Environ. Sci. 7 (2014) 812.

[8] A. Grytsiv, P. Rogl, H. Michor, E. Bauer, G. Giester, $In_yCo_4Sb_{12}$ skutterudite: phase equilibria and crystal structure, J. Electron. Mater. 42 (2013) 2940–2952.

[9] E. Visnow, C. P. Heinrich, A. Schmitz, J. de Boor, P. Leidich, B. Klobes, R. P. Hermann, W. E. M*ü*ller, W. Tremel, On the true indium content of In-filled skutterudites, Inorg. Chem. 54 (2015) 7818–7827.

[10] R. C. Mallik, J. Y. Jung, S. C. Ur, I. H. Kim, Thermoelectric properties of $In_zCo_4Sb_{12}$ skutterudites, Met. Mater. Int. 14 (2008) 223.

[11] M. Benyahia, V. Ohorodniichuk, E. Leroy, A. Dauscher, B. Lenoir, E. Alleno, High thermoelectric figure of merit in mesostructured $In_{0.25}Co_4Sb_{12}$ n-type skutterudite, J. Alloys Compd. 735 (2018) 1096–1104.

[12] J. Eilertsen, S. Rouvimov, M. Subramanian, Rattler-seeded InSb nanoinclusions from metastable indium-filled $In_{0.1}Co_4Sb_{12}$ skutterudites for high-performance thermoelectrics, Acta Mater. 60 (2012) 2178–2185.

[13] G. Li, K. Kurosaki, Y. Ohishi, H. Muta, S. Yamanaka, Thermoelectric properties of Indium-added skutterudites $In_xCo_4Sb_{12}$, J. Electron. Mater. 42 (2013) 1463.

[14] H. Li, X. Su, X. Tang, Q. Zhang, C. Uher, G. J. Snyder, U. Aydemir, Grain boundary engineering with nano-scale InSb producing high performance $In_xCe_yCo_4Sb_{12+z}$ skutterudite thermoelectrics, J Materiomics 3 (2017) 273–279.

[15] C. Chubilleau, B. Lenoir, C. Candolfi, P. Masschelein, A. Dauscher, E. Guilmeau, C. Godart, Thermoelectric properties of $In_{0.2}Co_4Sb_{12}$ skutterudites with embedded PbTe or ZnO nanoparticles, J. Alloys Compd. 589 (2014) 513–523.

[16] Y. Du, K. Cai, S. Chen, Z. Qin, S. Shen, Investigation on Indium-Filled Skutterudite Materials Prepared by Combining Hydrothermal Synthesis and Hot Pressing, J. Electron. Mater., year =.

[17] A. Gharleghi, P.-C. Hung, F.-H. Lin, C.-J. Liu, Enhanced ZT of $In_xCo_4Sb_{12}$-InSb nanocomposites fabricated by hydrothermal synthesis combined with solid-vapor reaction: a signature of phonon-glass and electron-crystal materials, ACS Appl. Mater. Interfaces 8 (2016) 35123–35131.

[18] S. Lee, K. H. Lee, Y.-M. Kim, H. S. Kim, G. J. Snyder, S. Baik, S. W. Kim,

Simple and efficient synthesis of nanograin structured single phase filled skutterudite for high thermoelectric performance, Acta Mater. 142 (2018) 8–17.

[19] M. S. Toprak, C. Stiewe, D. Platzek, S. Williams, L. Bertini, E. Müller, C. Gatti, Y. Zang, M. Rowe, M. Muhammed, The impact of nanostructuring on the thermal conductivity of thermoelectric $CoSb_3$, Adv. Funct. Mater. 14 (2004) 1189–1196.

[20] S. Le Tonquesse, E. Alleno, V. Demange, V. Dorcet, L. Joanny, C. Prestipino, O. Rouleau, M. Pasturel, Innovative one-step synthesis of mesostructured $CoSb_3$-based skutterudites by magnesioreduction, J. Alloys Compd. 796 (2019) 176–184.

[21] S. Le Tonquesse, V. Dorcet, L. Joanny, V. Demange, C. Prestipino, Q. Guo, D. Berthebaud, T. Mori, M. Pasturel, Mesostructure - thermoelectric properties relationships in $V_xMn_{1-x}Si_{1.74}$ (x = 0, 0.04) higher manganese silicides prepared by magnesiothermy, J. Alloys Compd. in press (2020) doi:10.1016/j.jallcom.2019.152577.

[22] W. Kroll, Verformbares Titan und Zirkon, Z. Anorg. Allg. Chem. 234 (1937) 42–50.

[23] F. H. Spedding, H. A. Wilhelm, W. H. Keller, Production of Uranium, U.S. Patent no. 2830894.

[24] E. Antolini, M. Ferretti, Synthesis and Thermal Stability of $LiCoO_2$, J. Solid State Chem. 117 (1995) 1–7.

[25] L. Ma, C. Y. Seo, X. Chen, K. Sun, J. W. Schwank, Indium-doped Co_3O_4 nanorods for catalytic oxidation of CO and C_3H_6 towards diesel exhaust, Appl. Catal. B-Environ. 222 (2018) 44–58.

[26] J. Rodriguez-Carvajal, Recent advances in magnetic-structure determination by neutron powder diffraction, Physica B 192 (1993) 55–69.

[27] O. Rouleau, E. Alleno, Measurement system of the Seebeck coefficient or of the electrical resistivity at high temperature, Rev. Sci. Instrum. 84 (2013) 105103.

[28] H. Toraya, Estimation of statistical uncertainties in quantitative phase analysis using the Rietveld method and the whole-powder-pattern decomposition method, J. Appl. Cryst. 33 (2000) 1324–1328.

[29] O. Knacke, O. Kubaschewski, K. Hesselmann, Thermo-chemical Properties of Inorganic Substances (1991) Springer Ed.

[30] B. P. de Laune, C. Greaves, Structural and magnetic characterisation of $CoSb_2O_4$ and the substitution of Pb^{2+} for Sb^{3+}, J. Solid State Chem. 187 (2012) 225–230.

[31] D. Larcher, A. S. Prakash, L. Laffont, M. Womes, J. C. Jumas, J. Olivier-Fourcade, M. S. Hedge, J.-M. Tarascon, Reactivity of antimony oxides and MSb_2O_6 (M = Cu,Ni,Co) trirutile-type phases with metallic lithium, J. Electrochem. Soc. 153 (2006) A1778–A1787.

[32] J. N. Reimers, J. E. Greedan, C. V. Stager, R. Kremer, Crystal structure and magnetism in $CoSb_2O_4$ and $CoTa_2O_6$, J. Solid State Chem. 83 (1989) 20–30.

[33] T. He, J. Chen, H. D. Rosenfeld, M. A. Subramanian, Thermoelectric properties of indium-filled skutterudites, Chem. Mater. 18 (2006) 759–762.

[34] S.-J. L. Kang, Sintering: densification, grain growth and microstructure (2004) Elsevier Ed.

[35] J. Eilertsen, Y. Surace, S. Balog, L. Sagarna, G. Rogl, J. Horky, M. Trottmann, P. Rogl, M. A. Subramanian, A. Weidenkaff, From occupied voids to nanoprecipitates: synthesis of skutterudite nanocomposites in situ, Z. Anorg. Allg. Chem. 641 (2015) 1495–1502.

[36] J.-Y. Jung, K.-H. Park, S.-C. Ur, I.-H. Kim, Thermoelectric and transport properties of In-filled $CoSb_3$ skutterudites, Mater. Sci. Forum 658.

[37] R. C. Mallik, C. Stiewe, G. Karpinski, R. Hassdorf, E. Müller, Thermoelectric properties of Co_4Sb_{12} skutterudite materials with partial In filling and excess In additions, J. Electron. Mater. 38 (2009) 1337–1343.

[38] A. Sesselmann, T. Dasgupta, K. Kelm, E. Müller, S. Perlt, S. Zastrow, Transport properties and microstructure of indium-added cobalt-antimony-based skutterudites, J. Mater. Res. 26 (2011) 1820–1826.

[39] J. Peng, X. Liu, L. Fu, W. Xu, Q. Liu, J. Yang, Synthesis and thermoelectric properties of $In_{0.2+x}Co_4Sb_{12+x}$ composite, J. Alloys Compd. 521 (2012) 141–145.

[40] V. V. Khovaylo, T. A. Korolkov, A. I. Voronin, M. V. Gorshenko, A. T. Burkov, Rapid preparation of $In_xCo_4Sb_{12}$ with a record-breaking ZT=1.5: the role of the In overfilling fraction limit and Sb overstoichiometry, J. Mater. Chem. A 5 (2017) 3541–3546.

[41] F. Chen, R. Liu, Z. Yao, Y. Xing, S. Bai, L. Chen, Scanning laser melting for rapid and massive fabrication of filled skutterudites with high thermoelectric performance, J. Mater. Chem. A 6 (2018) 6772–6779.

[42] K. Biswas, M. A. Subramanian, M. S. Good, K. C. Roberts, T. J. Hendricks, Thermal cycling effects on the thermoelectric properties of *n*-type In,Ce-based skutterudite compounds, J. Electron Mater. 41 (2012) 1615–1621.

[43] A. Sesselmann, B. Klobes, T. Dasgupta, O. Gourdon, R. Hermann, E. Müller, Neutron diffraction and thermoelectric properties of indium filled $In_xCo_4Sb_{12}$ (x = 0.05, 0.2) and indium cerium filled $Ce_{0.05}In_{0.1}Co_4Sb_{12}$, Phys. Status Sol. A 213 (2016) 766–773.

[44] L. Deng, L. B. Wang, J. M. Qin, T. Zheng, Effects of indium-filling and synthesis pressure on the thermoelectric properties of $CoSb_3$, Mod. Phys. Lett. B 28 (2014) 1450118.